Proceedings of the
International Conference on Mechanical Engineering and Renewable Energy 2013
(ICMERE2013) 1 – 3 May 2014, Chittagong, Bangladesh

ICMERE2013-PI-266

PENETRATION AND PERFORATION OF COMPOSITE STRUCTURES

Bazle Z. (Gama) Haque[1,*] and John W. Gillespie Jr.[2]

[1-2]Center for Composite Materials, University of Delaware, Newark, DE 19716, USA

[1,*] gama@udel.edu, Tel: +1 (302) 690-4741.

Abstract *- Penetration and perforation mechanics of composite laminates is investigated using explicit dynamic finite element analysis (FEA) code LS-DYNA. A rate dependent progressive composite damage model MAT162 in LS-DYNA is used in modeling different failure mechanisms of composites. Previously validated properties and parameters for plain-weave (PW) S-2 Glass/SC15 composite have been used for all computations. A right circular cylinder projectile has been taken as a baseline projectile. Numerical simulations have been conducted for a wide range of impact velocities covering both the non-perforating and perforating impact scenarios. Four phases of penetration, transition, perforation and retraction have been identified using the computational simulations and are presented.*

Keywords: Penetration & Perforation, Thin- & Thick-Section Composites, PW S-2 Glass/SC15, MAT162 in LS-DYNA, Ballistic Impact

1. INTRODUCTION

Perforation and penetration of metals, ceramics, rocks, and soils is a well-studied subject [1-4]. It is now well known that thin target perforates and thick or semi-infinite target penetrates [2]. Thickness dependent perforation and penetration damage modes of metals can be found [2, 3]. However, perforation and penetration of composite is a relatively new research area and is the main focus of the present paper. In Ref. [5], penetration and perforation of PW S-2 Glass/SC15 composites made from 11 layers (11L, 6.6-mm), 22L, & 33L of 814 gsm (24 oz/yd^2, 5×5 tows/in) plain-weave (PW) fabrics have been investigated both experimentally and numerically. In the present study we will present numerical simulations on penetration and perforation of a 52.8-mm thick 88L composite laminate. In addition we will also present perforation behavior of 4L, & 8L thin composite laminates. Numerical simulations are conducted using the explicit dynamic FEA code LS-DYNA and using the state-of-the-art progressive composite damage model MAT162.

2. FINITE ELEMENT ANALYSIS

FE model of a 2L square composite plate of dimensions 178-mm × 178-mm × 1.2-mm and stacking sequence $[0_2]$ is developed as one part with three (3) through-thickness brick elements. This 2L part is then stacked to develop the 4L ($[0_2/90_2]$), 8L ($[0_2/90_2]_2$), & 88L ($[0_2/90_2]_{22}$) FE models with different part numbers. Each alternating parts is assigned the material angle 0 or 90; such that there exist a pre-defined delamination plane between them. The in-plane mesh is finer in the center of the composite laminate while coarse elements are used at the boundaries [5-7]. Fig. 1 shows the top view and zoomed view of the composite laminate, cross-sections of the projectile and the composite laminates. A total number of 47.2k 3D solid elements have been used to model each 2L composite part, and total of 33.3 k 3D solid elements have been used to model the RCC projectile of mass, diameter, and length equal to 13.48-gm, 12.7-mm, 14.02-mm; respectively. To simplify the problem, all four edges of the composite laminate are constrained for all translations and rotations. A single surface contact definition with high friction is used followed by the methodology described in Ref. [5].

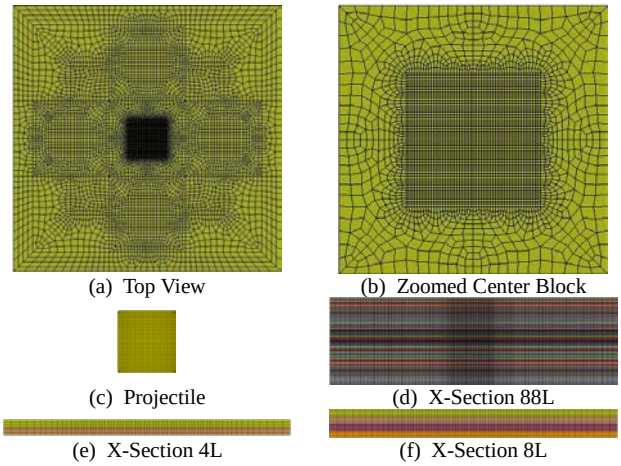

(a) Top View (b) Zoomed Center Block (c) Projectile (d) X-Section 88L (e) X-Section 4L (f) X-Section 8L

Fig. 1. 3D FEM of the 4L, 8L, & 88L PW S-2 Glass/SC15 Composite Laminates with the RCC Projectile. (Not in Scale).

Elastic properties of steel (ρ = 7.85 g/cm^3, E = 210 GPa, & ν = 0.30) are used to model the projectile. The required input for the PW S-2 glass/SC15 composite material to the MAT162 composite damage model are taken from our previous work [5], presented in Appendix A, and the details of MAT162 can be found at the UD-CCM website [8].

3. RESULTS AND DISCUSSION

3.1 Penetration and Perforation Mechanisms of a Thick Composite Laminate [6]

From the LS-DYNA simulations below and above the ballistic limit velocity (complete penetration with zero projectile residual velocity) of the 88L composite plate, four phases of penetration mechanisms are identified as: (i) the penetration phase or P-Phase, (ii) the transition phase or T-Phase, (iii) the perforation phase or F-Phase, and (iv) the retraction or R-Phase. Characteristics of these phases are described below.

3.1.1 The Penetration Phase or P-Phase

The penetration damage mechanisms below and above the ballistic limit is investigated by observing the cross-section of the composite laminate at different times, as presented in Fig. 2, which shows penetration of the projectile into the composite target till time t = 30 μs due to the crush failure of composites under the projectile and erosion of the compressed/crushed elements when their final volume to initial volume ratio is 0.001.

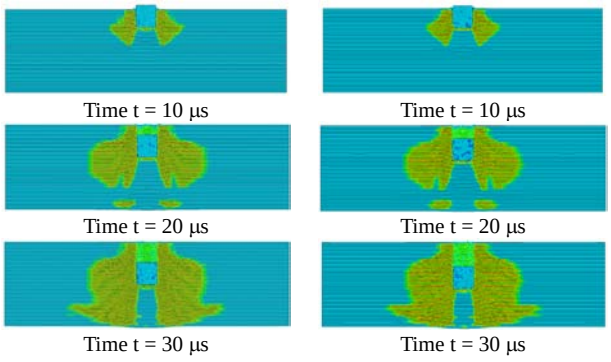

Fig. 2: Penetration or P-Phase of a 88L thick PW S-2 Glass/SC15 composite laminate.

Transverse matrix damage and delamination around the depth of penetration cavity is observed, however, no matrix cracking or delamination damage is visible under the projectile, nor any visible dynamic deflection of the back face lamina, except at t = 30 μs, where initiation of delamination is visible between the last two sub-laminates at the back face. Initiation of delamination between the last two sub-laminates is caused by the tensile wave reflection from the free back face, and this event is attributed to the end of the penetration or P-Phase. During the P-Phase, the composite material surrounding the projectile shows some bending deformation in the same direction to the projectile motion; however, the relative velocity between the projectile and its surrounding composite material is very small and can be assumed to be zero. This observation reveals the fact that during P-Phase the relative velocity between the projectile and the surrounding composite is negligible or can be assumed to be zero for all practical modeling purposes. In reality, the crushed composite under the projectile during the P-Phase is ejected from the penetration cavity in a direction opposite to the projectile motion, and is not captured in the numerical simulation because of the numerical erosion criteria.

3.1.2 The Transition Phase or T-Phase

Transition or T-Phase starts at the end of the P-Phase. The projectile continues to penetrate while the composite under the projectile is under intense compression-shear while the composites surrounding the projectile undergo transverse shear deformation. As an outcome, transverse matrix damage and delamination forms a zone of damaged material, which can be termed as the damaged cone, and the composite under and surrounding the projectile in the damage cone undergo dynamic deformation. At certain point of time, penetration of the projectile into the composite ceases, and the composite under the projectile achieves the same particle velocity as the projectile, and this phenomenon is marked as the end of the Transition or T-Phase (Fig. 3). The end of T-Phase is found to occur around t = 70 μs & t = 60 μs for the 1300 m/s & 1400 m/s impact cases, respectively.

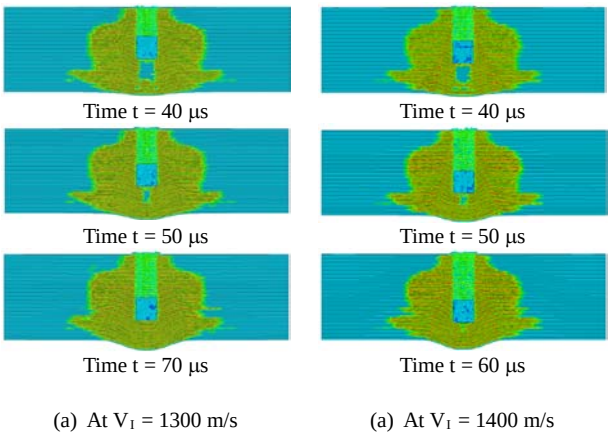

Figure 3: Transition or T-Phase of a 88L thick PW S-2 Glass/SC15 composite laminate.

3.1.3 The Perforation Phase or F-Phase

The end of the Transition or T-Phase marks the beginning of the Perforation or F-Phase. In addition, the appearance of the first tension-shear damage mode in the damage cone is also attributed to the beginning of the Perforation or F-Phase. Since the projectile and the composite in contact under it moves together with the same particle velocity, i.e., the relative velocity between them is zero; the F-Phase can be considered as quasi-static, and thus energy and momentum based theoretical models can be developed to study this phase of deformation. During the F-Phase, composite materials under the projectile undergo compression-shear loading while the surrounding damage cone undergoes tension-shear loading. Our

previous experimental work on Quasi-Static Punch Shear Test (QS-PST) experimental methodology have identified that during quasi-static penetration a shear-plug is formed under the projectile which pushes the material ahead of it, which fails under tension shear or in other words, perforates the composite, and the shear-plug is ejected through the perforation cavity. Similar plug-formation, perforation of the back face laminas, and ejection of the plug are also observed in the numerical simulation presented in Fig. 4. The back-face dynamic deflection reaches its absolute maximum and marks the end of the Perforation or F-Phase.

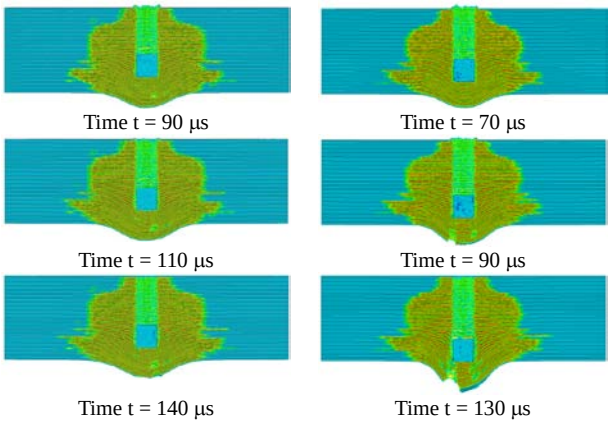

(a) At V_I = 1300 m/s (a) At V_I = 1400 m/s

Figure 4: Perforation or F-Phase of a 88L thick PW S-2 Glass/SC15 composite laminate.

3.1.3 The Retraction Phase or R-Phase

At the point of maximum dynamic deflection of the back face, the particle velocity of the last sub-laminate at the peak-deflection point becomes zero, the particle velocity reverses its direction of motion, and the last sub-laminate and the remaining laminates starts retracting back and marks the beginning of the Retraction or R-Phase. At the beginning of the R-Phase, the absolute velocity of the projectile may not be zero; rather it can be positive such that the projectile continues to move forward. In case of impact velocities above the ballistic limit, the above mentioned hypothesis is definitely true, as the projectile continues to move forward and ejects from the perforation cavity with positive definite residual velocity along the direction of projectile motion. In case of an impact velocity less than the ballistic limit, the projectile comes to a stop and reverses its direction and rebounds while the remaining non-perforated section of the composite laminate retracts back.

3.1.4 Depth of Penetration and Back-Face Dynamic Deflection during P-Phase, T-Phase, and F-Phase Phases

Fig. 6 shows the dimensionless Z- & X-coordinates of the top and bottom layer of the composite plate for two different impact velocities, i.e., at 1300 m/s, and at 1400 m/s. End of P-Phase, T-Phase, and F-Phase is presented, which clearly shows the depth of penetration and the dynamic deflection of the back face at the end of each phases from the top face coordinates.

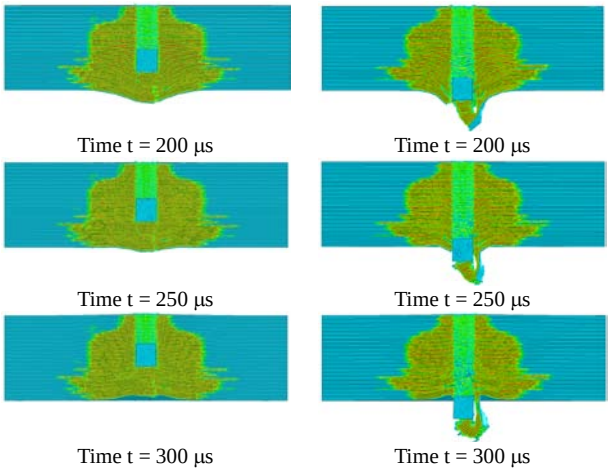

(a) At V_I = 1300 m/s (a) At V_I = 1400 m/s

Figure 5: Retraction or R-Phase of a 88L thick PW S-2 Glass/SC15 composite laminate.

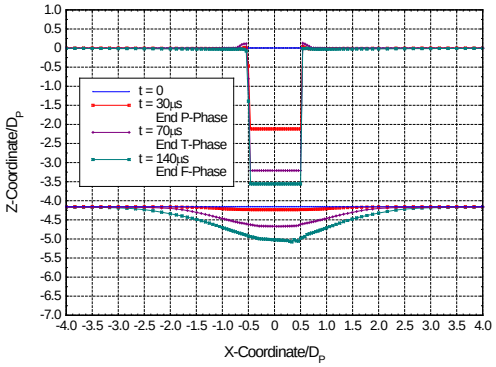

(a) Below ballistic limit at V_I = 1300 m/s

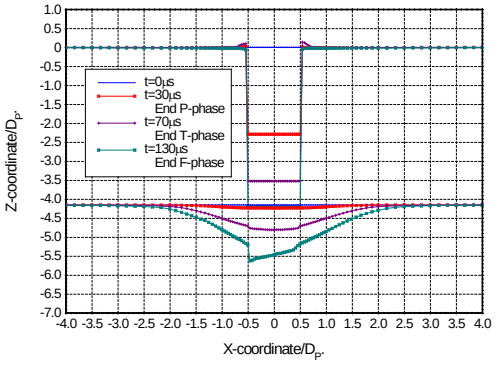

(b) Above ballistic limit at V_I = 1400 m/s

Fig. 6: Depth of penetration and back-face dynamic deflection during P-Phase, T-Phase, and F-Phase Phases.

3.2 Perforation Mechanisms of Thin Composite Laminates [7]

Following the four different penetration phases of thick composites, a thin laminate can be defined as a laminate which does not show any penetration (P-Phase) or transition (T-Phase) phases, rather show only the perforation (F-Phase) and retraction (R-Phase) phases.

Dynamics of thin composite perforation has been evaluated at two different impact velocities, i.e., (i) below ballistic limit & rebound, and (ii) above ballistic

limit & perforation. Because of the jump near the ballistic limit velocity, the below and above ballistic limit velocities are chosen such that the chosen impact cases represent pure rebound or pure perforation. Figs. 7 and 8 show the snapshots of dynamic deformation of the 4L and 8L laminates impacted below and above their respective ballistic limit velocities.

3.2.1 Characteristics of the Perforation or F-Phase

From Figs. 7 and 8, in the perforation phase or F-Phase, no penetration of the laminate is observed. In the F-Phase, the laminates show a global bending deformation with a local large deformation damage zone. The global bending reaches the edge of the plate and reflects back even before the end of perforation or F-Phase. The end of the F-Phase is marked by the first trace of retraction of the laminate (defined in the next section).

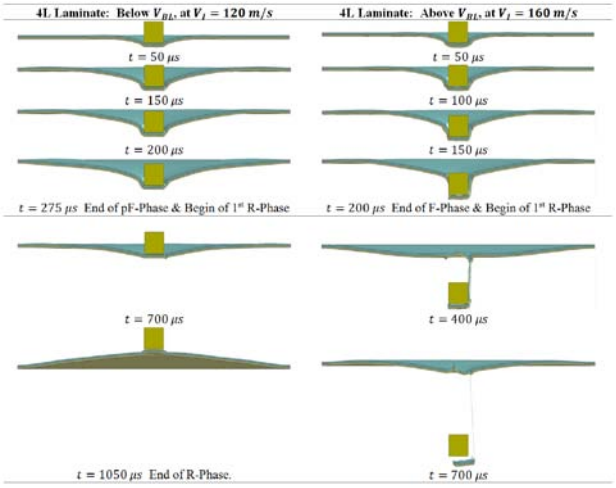

Fig. 7: Perforation (F-Phase) and Retraction (R-Phase) Phases of 4L Composite Plate below and above the Ballistic Limit Velocity.

For impact velocities lower than the ballistic limit velocity, the perforation (F-Phase) phase can be termed as pre-perforation or pF-Phase. The dynamics of pF-Phase clearly shows what happens before perforation. For impact velocities higher than the ballistic limit velocity, at the end of the perforation (F-Phase) phase, the laminate perforates; however, perforation process is progressive in nature. The large deformation perforation process is local to the periphery of the projectile, and the dominant damage mechanism is combined tension-shear. The formation of a local tension-shear damage zone is evident in case of the 8L composite laminate.

3.2.2 Characteristics of the Retraction or R-Phase

At the end of the perforation or F-Phase, a portion of the composite plate near the projectile starts moving in a direction opposite to the impact direction of the projectile and marks the end of F-Phase or pF-Phase and the beginning of the retraction or R-Phase.

For most ballistic limit analysis, R-Phase is not important, because the stored kinetic energy in the laminate will dissipate via long time vibration and damping. For non-perforating pF-Phase, the beginning of retraction phase is somehow related to the rebound of the projectile, and it is justified to define the end of pF-Phase and the beginning of R-Phase when the projectile rigid body velocity is zero.

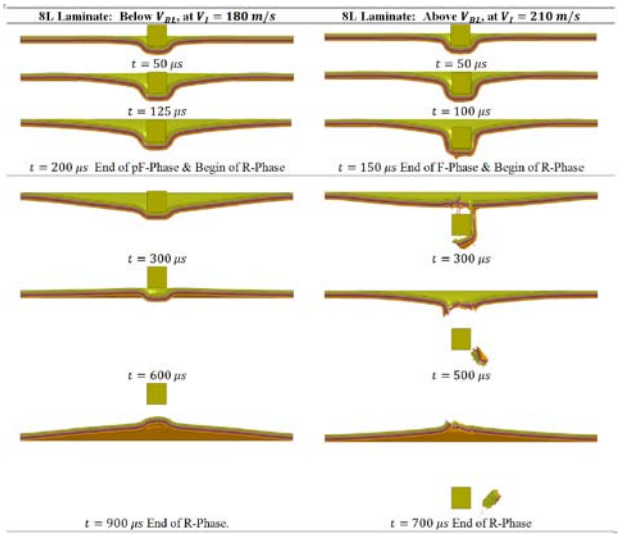

Fig. 8: Perforation (F-Phase) and Retraction (R-Phase) Phases of 8L Composite Plate below and above the Ballistic Limit Velocity.

3.2.3 3D Displacement-Time-Location Plots for pF-Phase and F-Phase

The pre-perforation (pF-Phase) and the perforation (F-Phase) phases of the 4L and 8L composite laminates have further been investigated using the 3D plot of Displacement, Time, and Location at a cross-section on the top and bottom surface of the laminate. Figs. 9 and 10 show these 3D plots. For a thin laminate, the deformation of the top and bottom surface can be considered approximately the same.

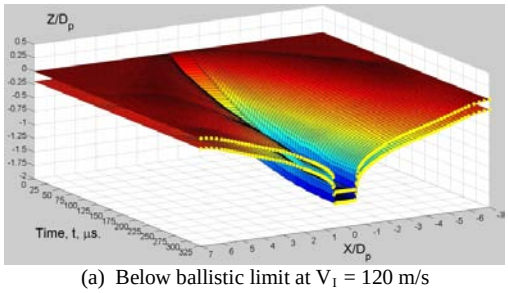

(a) Below ballistic limit at V_I = 120 m/s

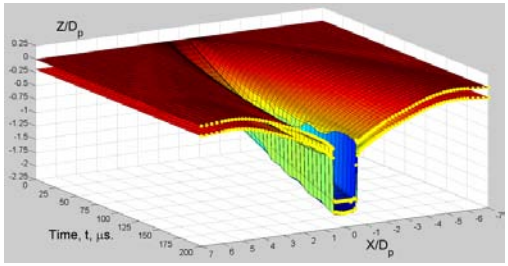

(b) Above ballistic limit at V_I = 160 m/s

Fig. 9: 3D Displacement-time-location plots of pF-Phase and F-Phase for 4L composite plate.

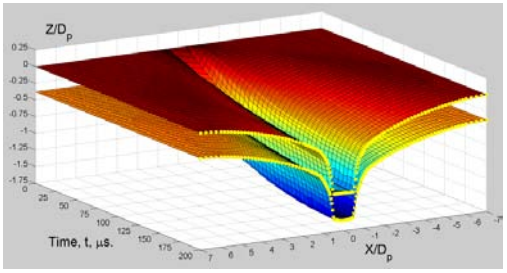

(a) Below ballistic limit at V_I = 180 m/s

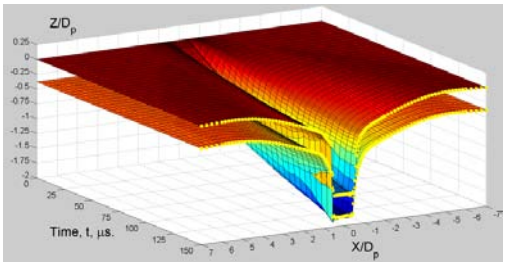

(b) Above ballistic limit at V_I = 210 m/s

Fig. 10: 3D Displacement-Time-Location Plots of pF-Phase and F-Phase for 8L Composite Plate.

4. SUMMARY

Based on a previously validated composite damage model of PW S-2 Glass/SC15 composites, LS-DYNA simulations on thick-section composite plates have identified four penetration phases, namely, (i) The Penetration or P-Phase, (ii) the Transition or T-Phase, (iii) the Perforation or F-Phase, and the less important (iv) Retraction or R-Phase. In addition, a thin laminate is differentiated form a thick laminate by the fact that for a thin-laminate, the P-Phase and T-Phase are absent. Computational simulation shows that a 4L (2.4-mm) and a 8L (4.8-mm) composite plate shows only perforation or F-Phase, and the retraction or R-Phase of deformation.

While the dynamics of penetration and perforation can be found in our previous publications [6, 7], the dynamic deformation and damage mechanisms of both thick- and thin-section composites are presented here. Depending on the composite plate thickness-to projectile diameter ratio, it has been identified that the mechanics of penetration and perforation is dependent on the composite thickness for a projectile with constant diameter and length.

The present study sets the background for further analysis on the effect of projectile diameter and length on penetration mechanisms and for developing theoretical models for different penetration phases.

6. ACKOWLEDGEMENT

Research was sponsored by the Army Research Laboratory through the Composite Materials Research program in developing the composite damage modeling methodologies. The views and conclusions contained in this document are those of the authors and should not be interpreted as representing the official policies, either expressed or implied, of the Army Research Laboratory or the U. S. Government. The U. S. Government is authorized to reproduce and distribute reprints for Government purposes notwithstanding any copyright notation hereon.

Contributions of undergraduate students Jessica Harrington, Richard Stanton, and graduate intern Ishita Biswas in performing the LS-DYNA simulations and extracting results are gratefully acknowledged.

7. REFERENCES

[1] Carlucci, D. E., and Jacobson, S. S., "BALLISTIC: Theory and design of guns and ammunition." CRC Press Taylor & Francis Group, 2008.

[2] Goldsmith, W., "IMPACT: The theory and physical behavior of colliding solids." Edward Arnold (Publishers) Ltd., 1960. Republication by Dover Publications, Inc. Mineola, NY, 2001.

[3] Backman, M. E., and Goldsmith, W., "The mechanics of penetration of projectiles into target." International Journal of Engineering and Science, 1978, Vol. 16, pp. 1-99.

[4] Ben-Dor, G., Dubinsky, A., and Elperin, T. (2006). Applied High-Speed Plate Dynamics. Springer.

[5] Gama, B. A., and Gillespie, J. W., "Finite Element Modeling of Impact, Damage and Penetration of Thick-Section Composites," International Journal of Impact Engineering, 2011, Vol. 38, pp. 181-197.

[6] (Gama) Haque, B. Z., Harrington, J. L., Biswas, I., and Gillespie Jr., J. W. "Perforation and Penetration of Composites." CD Proceedings, SAMPE 2012 Baltimore, MD. May 21-24, 2012.

[7] (Gama) Haque, B. Z., Stanton, R. J., and Gillespie Jr., J. W. "Perforation Mechanics of Thin Composites." CD Proceedings, SAMPE 2013 Long Beach, CA. May 6-9, 2013.

[8] http://www.ccm.udel.edu/Tech/MAT162/

8. APPENDIX A

MAT162 Input Properties and Parameters for PW S-2 Glass/SC15 Composite, adopted from Ref. [5]

MID	RO, kg/m³	EA, GPa	EB, GPa	EC, GPa	PRBA	PRCA	PRCB
162	1850.00	27.50	27.50	11.80	0.11	0.18	0.18
GAB, GPa	GBC, GPa	GCA, GPa					
2.90	2.14	2.14					
SAT, MPa	SAC, MPa	SBT, MPa	SBC, MPa	SCT, MPa	SFC, MPa	SFS, MPa	SAB, MPa
604.00	291.00	604.00	291.00	58.00	850.00	300.00	75.00
SBC, MPa	SCA, MPa	SFFC	PHIC	E_LIMT	S_DELM		
58.00	58.00	0.300	10	0.200	1.200		
OMGMX	ECRSH	EEXPN	CRATE1	AM1			
0.999	0.001	4.500	0.030	2.00			
AM2	AM3	AM4	CRATE2	CRATE3	CRATE4		
2.00	0.50	0.20	0.000	0.030	0.030		